

2 mil

THE UNIVERSITY OF MICHIGAN
COLLEGE OF ENGINEERING

Departments of Aerospace Engineering
Atmospheric and Oceanic Science
High Altitude Engineering Laboratory

(NASA-CR-124348) MEASUREMENTS OF THE
MICHIGAN AIRGLOW OBSERVATORY FROM 1971 TO
1973 AT ESTER DOME ALASKA Final
Technical Report (Michigan Univ.) 4/ 40 p
HC \$4.00

N73-30351

Unclass
CSCL 04A G3/13 15381

Final Technical Report

MEASUREMENTS OF THE MICHIGAN AIRGLOW OBSERVATORY
FROM 1971 TO 1973 AT ESTER DOME, ALASKA

K. D. McWatters
J. W. Meriwether
P. B. Hays
A. F. Nagy

ORA Project 011017



under contract with:

NATIONAL AERONAUTICS AND SPACE ADMINISTRATION
GEORGE C. MARSHALL SPACE FLIGHT CENTER
CONTRACT NO. NSA 8-28592

administered through:

OFFICE OF RESEARCH ADMINISTRATION

ANN ARBOR

June 1973

TABLE OF CONTENTS

	Page
ABSTRACT	1
INTRODUCTION	2
INSTRUMENTATION	3
GEOPHYSICAL RESULTS	6
CONCLUSIONS	10
REFERENCES	12
TABLE I	14
LIST OF FIGURES	15
APPENDIX A	34

ABSTRACT

The Michigan Airglow Observatory (MAO) has been located at Ester Dome Observatory, College, Alaska (Latitude: $64^{\circ}53'N$, Longitude: $148^{\circ}03'W$) since October, 1971. The MAO houses a 6-inch Fabry-Perot interferometer, a 2-channel monitoring photometer and a 4-channel tilting filter photometer. The Fabry-Perot interferometer has been used extensively during the winter observing seasons of 1971-72 and 1972-73 to measure temperature and mass motions of the neutral atmosphere above ≈ 90 kilometers altitude. Neutral wind data from the 1971-72 observing season as measured by observing the Doppler shift of the $\lambda 6300 \text{ \AA}^{\circ}$ atomic oxygen emission line are presented in this report. Summaries of the work for each year may be found in Appendix A.

INTRODUCTION

The Michigan Airglow Observatory (MAO) has been located at Ester Dome Observatory, College, Alaska (Latitude: $64^{\circ}53'N$, Longitude: $148^{\circ}03'W$) since October, 1971. The MAO houses a 6-inch Fabry-Perot interferometer, a 2-channel monitoring photometer and a 4-channel tilting filter photometer (Figure 1). The Fabry-Perot interferometer has been used extensively during the winter observing seasons of 1971-72 and 1972-73 to measure temperature and mass motions of the neutral atmosphere above ≈ 90 kilometers altitude. Neutral wind data from the 1971-72 observing season as measured by observing the Doppler shift of the $\lambda 6300 \text{ \AA}$ atomic oxygen emission line are presented in this report. Summaries of the work for each year may be found in Appendix A.

The measurement of the Doppler broadening of the $\lambda 6300 \text{ \AA}$ atomic oxygen emission line ($O(^1D)-O(^3P)$) provides an excellent source of direct information on upper atmospheric temperatures in the F-region (Biondi and Fiebelman, 1968; Hays, Nagy and Roble, 1969; Armstrong, 1969). If the radiating atoms are in thermal equilibrium with the parent gas, then ambient (kinetic) temperatures may be deduced. Similar measurements of the $\lambda 5577$ OI line will provide temperature information in the E-region. The technique employed to obtain temperatures and Doppler shifts from the interferometer data has been described (Hays and Roble, 1971).

The importance of dynamics in controlling the physical behavior of the upper atmosphere has been well established during the last few years. The role of the diurnal winds has been studied theoretically (e.g., Kohl and King, 1967; Geisler, 1967; Challinor, 1969; Friedman, 1970) and experimentally (e.g. Armstrong, 1969; Hays and Roble, 1971). The Doppler shift of the $\lambda 6300$ OI line leads to measurement of F-region neutral winds. It has

been shown that during magnetic storms, heating takes place at high latitudes (Blamont and Luton, 1970; Tausch, Carignan and Reber, 1970) and that strong equatorward winds result (Hays, et. al., 1969; Meriwether et. al, 1973), which are certainly part of a large meridional circulation pattern set in motion by the storm. It is, therefore, of great importance to learn as much about the wind system as possible.

INSTRUMENTATION

The six inch Fabry-Perot interferometer has been described in detail (Roble, 1969; Hays, Nagy and Roble, 1969) and thus, only a brief discussion of the modifications will be included here. A summary of the Fabry-Perot interferometer operating parameters is given in Table I. The optical section, where the pre-filtering takes place (Figure 2), has been modified so that filters can be changed remotely, allowing rapid changes of the line being observed. The method of scanning a line profile with the interferometer was changed to a discrete density scan mode for the 1972-73 observing season. The ability to scan with this mode has improved the ability of the Fabry-Perot to measure the Doppler shift of weak emission lines and consequently, the neutral wind. A wavelength shift associated with a line-of-sight speed of 1 m/sec is about $2 \times 10^{-5} \text{ \AA}$, which corresponds to a pressure change in the etalon chamber of about $2 \times 10^{-4} \text{ psi}$, when nitrogen is used as the scanning gas. Consequently, to determine line positions accurately, one requires a very precise pressure monitor and if possible, the ability to make pressure shifts equivalent to the Doppler line width quickly and repeatedly. A closed, discrete density scanning system was constructed, which allows rapid changes in wavelength with an accuracy of about $3 \times 10^{-5} \text{ \AA}$. This is accomplished by using a piston to change the volume of the system which

contains a fixed amount of gas. This system is illustrated in a block diagram in Figure 3. The ability to scan using the older linear scan mode was also maintained.

This new instrumentation was used during the 1972-73 observing season to measure the line position and Doppler width by monitoring the emission feature at the following five precise wavelength positions: two points in the far wings of the line, one measurement at the half height position on each side of the line and one measurement at the line center. This waveform was supplemented by two background measurements at positions isolated from the emission. The line-of-sight wind speed determined by this technique will be accurate to within the value:

$$\delta W = \frac{\alpha}{\sqrt{N_{\text{peak}}}}$$

where α depends upon the line width ($\alpha = 1000$ m/sec for the red line) and N_{peak} is the number of counts accumulated at the line center. Thus, for the red line we achieve a basic sensitivity of about 10 m/sec with a 1 kR intensity and 20 sec integration period.

A new 4-channel tilting filter photometer was installed in October, 1971. This photometer operates under a different mirror system than the interferometer and can scan an emission feature in the conventional manner (Eather and Reasoner, 1969) or the pass band can be shifted between the emission line and the background. The tilting filter photometer may be used as a meridian scanning photometer or a monitoring photometer. During the 1971-72 observing season, the 4-channel tilting filter photometer was used mainly to monitor the emission feature being observed by the interferometer. The photometer data could then be used to normalize the interferometer data for times of considerable intensity variations.

A new 2-channel monitoring photometer was installed for the 1972-73 observing season under the interferometer mirror system. This photometer has the same field of view as the interferometer and is optically aligned with the interferometer. The monitoring photometer simply monitors the overall intensity of the emission feature being observed and is used to normalize the interferometer data. The installation of the 2-channel monitoring photometer has acted to free the 4-channel tilting filter photometer for general auroral survey work.

GEOPHYSICAL RESULTS

A) Neutral Wind Measurements

The main purpose of the MAO observations from College, Alaska, for the 1971-1972 and 1972-1973 observing seasons was to determine the relationship of the neutral circulation pattern to polar convection and auroral particle precipitation. Figures 4-14 present neutral wind vectors for those nights for which the coverage with respect to local time was reasonably complete. In addition to the neutral wind data, magnetic activity for each night is shown by the College magnetogram and K_p indices. The neutral wind vectors were based upon individual measurements in each of the four cardinal geomagnetic directions in addition to zenith measurements. The latter set was used to provide a zero shift reference with the assumption of a zero vertical wind. By using four cardinal compass points rather than the minimum three required for a vector determination, it was possible to determine the importance of gradients in the neutral wind flow.

Figure 15 portrays the collection of the central pressure measurements for all of the fringes obtained for various look angles on the night of March 2, 1971. The central pressure of the fringes (Hays and Roble, 1971) is a measure of the Doppler shift of the line profile with respect to a reference, which was obtained by an eyeball fit to the sequence of zenith measurements. The difference between the central pressure of a particular fringe and the reference is a measure of the line of sight velocity for the direction chosen, where a shift of the fringe peak of .01 psi is equivalent to 55 m/s (Hays and Roble, 1971). The data for each wind component, (N-S or E-W) are plotted and fitted by eye. The dashed lines in Figure 15 labeled $+\sigma$ and $-\sigma$ indicate the standard deviation of the scatter in the line of sight speed with respect to the fitted line. Figure 16 shows how the March 2 points fall with respect to this curve for both the E-W and the N-S measurements. This procedure involves two assumptions; namely, one, that the

vertical wind is negligible with respect to the horizontal wind and two, the gradient of the neutral wind across 400 km (a typical scale size for these measurements) would be negligible. The 71/72 data indicate that these assumptions appear to be valid within the stability limitations of the interferometer, estimated to be equivalent to ± 30 -40 m/s. However, the preliminary data obtained from the 72/73 observations with the discrete density scan mode, where the stability is considerably better, appears to indicate that both assumptions need re-evaluation, but within the limits of ± 50 m/s no modifications to this method of data treatment need to be made. Careful study was given to each assumption in the last observing season, and the high precision of these measurements coupled with better temporal resolution will determine these limits more accurately.

One particular aspect of neutral wind measurements from line profiles that need to be kept in mind is the altitude of the emission. Normally for airglow the emission originates from the F-layer in a region where the neutral wind vector ceases to rotate with altitude so that the fringe represents an integration along the emission profile of roughly 30 to 50 km in breadth within which the direction of the neutral wind vector is constant. In auroras the hardness of the flux of precipitating particles shifts the profile to lower altitudes where the possible range of neutral wind directions might be 15 - 20° or greater. The barium cloud releases and TMA trails from College, (Meriwether et. al., 1973) as well as at other sites indicate the directional shifts to be small for altitudes of 170 km or higher. Thus, the lack of knowledge concerning the centroid does not appear to be very critical for the set of measurements reported here. The temperature measurements permit some feeling as to what the actual emission height might be, and results obtained give values ranging from 800°K to 900°K in most conditions; from this it is concluded that generally the emission height is clearly above 170 km.

B) Ion Drift Measurements

If the emission used for a source originates from an ion rather than neutral atomic oxygen, for example, the atomic oxygen ion, then a sequence of Doppler shift measurements based upon line profile positions with respect to a reference provide information about ion drifts in the thermosphere, assuming thermal equilibrium of the ion. The O^+ emission of $\lambda 7319$ provides a suitable candidate to fulfill this role of a source as the lifetime of five seconds not only allows sufficient time for thermal equilibrium, but also leads to emission coming only from the F-layer as quenching eliminates this state before emission within the lower thermosphere. Figure 17 shows two fringes obtained during a negative bay on February 12, 1971 (UT) within a twenty minute period. The Doppler shifts displayed in this figure, assuming no horizontal gradient in the ion drift, are equivalent to a drift speed of 1000 m/s to the east which implies a southward electric field of 40 volts/km in accord with the presence of a 750 Δ negative bay.

Although it has been demonstrated that this technique produces results that are typical of barium release measurements (Wescott et.al., 1969), incoherent scatter radar (Doupnik et.al., 1972), and spacecraft probes (Cauffman and Gurnett, 1972), the morphology of the $\lambda 7319$ emission was found to be erratic and spotty with respect to typical observing conditions and, in addition, even in the best of conditions, the emission intensity was less than 200R so that long integration times were required for an adequate measurement.

C) Temperature Profile Measurements of an Arc

Temperature measurements obtained as a by-product of neutral wind measurements were not as geophysically interesting as height measurements are required for the proper interpretation of temperatures obtained from auroral emissions. The results are of some value for interpretation of the origin of the emission as a high temperature infers a high altitude emission and a low temperature infers a low altitude emission.

— One arc profile sequence of measurements in $\lambda 5577$ was taken in conjunction with the meridian scanning photometers at Ester Dome, Alaska, and Ft. Yukon, Alaska. The results are shown in Figure 18 in addition to the Jacchia 1971 model atmosphere temperature profiles. Ion temperatures were obtained during the same event by the incoherent scatter radar and are also presented in Figure 18. The measurements were taken in a limited time span caused by the short lifetime of an arc. Consequently, the poor statistics created by the need for rapid measurements lead to considerable error in the temperature values, typically $\pm 50^\circ\text{K}$. The error was computed in accord with the formulae presented in Hays and Roble (1971) with modifications arising from the lower reflectivity of the plates at $\lambda 5577$ and the narrower width of its line profile in comparison with the $\lambda 6300$ case.

The breadth of the aurora within the interferometers' field of view also generates uncertainty. Figure 18 presents the best estimates of the height which were based upon photometer scans from Ester Dome and Ft. Yukon. Both the temperature and error estimates are indicated by the error bars in Figure 18. The results are inconclusive as the degree of error is such that there is little departure from the model atmosphere temperature profiles, although there is some indication that the ion temperatures tended to fall lower than the model in the height region of 150 km. This latter

feature may be explained on the basis of a poor model ionosphere used for temperature retrieval from the ion Doppler profile obtained with the incoherent scatter technique.

CONCLUSIONS

A definite pattern in the local time dependence of the neutral wind direction at high latitudes during moderately disturbed conditions is shown by the data in this report. This pattern is supported by a "quick-look" preliminary analysis of data obtained during the 1972-73 observing season. Chief characteristics of this pattern is a wind to the west in the early evening hours followed by a strong wind to the south that normally peaks near 0300-0400 local time. The E-W wind component for the post midnight hours tends to be considerably smaller in magnitude as compared with the early evening hours, and the wind direction highly variable from night to night. A strong disagreement exists between the observed winds characterized by this pattern and the calculated winds derived from global pressure fields (e.g. Challinor, 1970). The disagreement might be attributed to several factors. One is the decreased importance of day-to-night neutral flow across the terminator resulting from solar heating. The lower speed of this flow might be attributed to the low solar elevation angles during the winter season suggesting that the sun plays a much lesser role in driving the atmosphere at high latitudes than at low latitudes.

Another important consideration for the origin of neutral wind flow at high latitudes is the presence of an ion convection pattern above the plasmopause. Typically, the direction of the zonal wind arising from ion drag induced by ion drifts would be to the west in early evening and to the east in early morning. Associated with the convection would be considerable

heating arising from joule heating due to Pedersen currents and from particle deposition of energy in auroras. Both would create a southward wind in the course of expansion in the cellular upwelling generated by the heating. Thus, the mechanisms of ion drag and polar heating can be combined to generate a neutral wind pattern that has the same features as that observed.

Quantitative study by means of modeling is highly desirable for further progress. Cooperative measurements with the Chatanika incoherent radar facility located near College, Alaska (Leadabrand, 1972) have been undertaken in both the past two seasons, but most notably in February and March, 1973 (Nagy et.al., 1973) when a strong effort was made to make simultaneous measurements with the radar. Simultaneous acquisition of neutral mass motion as obtained by MAO and ion mass motion as obtained by the radar is needed as inputs for the quantitative modeling. From these cooperative studies, it should be possible to establish the relative roles that ion drag, day-to-night pressure gradient, and polar heating play in the generation of the neutral wind at high latitudes.

REFERENCES

- Armstrong, E. P., "Doppler Shifts in the wavelength of the OI 6300 line in the night airglow", Planet. Space Sci., 17, 957, 1969.
- Biondi, M. A. and Feibelman, W. A., "Twilight and nightglow spectral line shapes of oxygen 6300 and 5577 radiation", Planet. Space Sci., 16, 431, 1968.
- Blamont, J. E. and Luton, J. M., "OGO-VI direct measurement of the temperature of the neutral atmosphere from 200 km to 350 km of altitude", Space Res. XI, 1970.
- Cauffman, D. P. and Gurnett, D. A., "Satellite measurements of high latitude convection electric fields", Space Sci. Rev., 13, 369, 1972.
- Challinor, R. A., "Neutral-air winds in the ionospheric F-region for an asymmetric global pressure system", Planet. Space Sci., 17, 1097, 1969.
- Doupnik, J. R., Banks, P. M., Bacon, M. J., Rino, C. L., and Petriceks, J., "Direct measurements of plasma drift velocities at high magnetic latitudes", J. Geophys. Res., 77, 4268, 1972.
- Eather, R. H. and Reasoner, D. L., "Spectrophotometry of faint light sources with a tilting filter photometer", Appl. Optics, 8, 227, 1969.
- Friedman, M. P., "Upper atmosphere dynamics", Smithsonian Astrophysical Observatory Special Report 316, 1970.
- Geisler, J. E., "A numerical study of the wind system in the middle thermosphere", J. Atmos. Terr. Phys., 29, 1469, 1967.
- Hays, P. B., Nagy, A. F. and Roble, R. G., "Interferometric measurements of the 6300 A doppler temperature during a magnetic storm", J. Geophys. Res., 74, 4162, 1969.
- Hays, P. B., McWatters, K.D., Roble, R. G. and Nagy, A. F., "Interferometer measurements of upper atmospheric temperatures and winds", paper presented at the Fall AGU Meeting, San Francisco, 1969.
- Hays, P. B. and Roble, R. G., "Direct observations of thermospheric winds during geomagnetic storms", J. Geophys. Res., 76, 5316, 1971.
- Kohl, H. and King, J. W., "Atmospheric winds between 100 and 700 km and their effects on the ionosphere", J. Atmos. Terr. Phys., 29, 1045, 1969.
- Meriwether, J. W., Heppner, J. P., Stolarik, J. D. and Wescott, E. M., "Neutral winds above 200 km at high latitudes", J. Geophys. Res., 78, 1973 (in press).

Roble, R. G., "A theoretical and experimental study of the stable mid-latitude red arc (sar-arc)", Ph. D. Thesis, University of Michigan 1969.

Taeusch, D. R., Carignan, G. R. and Reber, C. A., "Response of the neutral atmosphere to geomagnetic disturbances", Space Res. XI, 1970.

Wescott, E. M, Stolarik, J. D. and Heppner, J. P., "Electric fields in the vicinity of auroral forms from motions of barium vapor releases", J. Geophys. Res., 74, 3469, 1969.

TABLE I.

OPERATING PARAMETERS OF THE FABRY-PEROT INTERFEROMETER

1. Etalon plates	
effective diameter	5-1/4"
flatness	$\lambda / 180$
roughness defect, N_{Dg}	40
reflective coatings	5 alternate layers of ZnS and cryolite
reflectivity	0.87 at 6300 Å
reflective finesse, N_R	23
spherical defect finesse, N_{Df}	20.3
sagitta	1.55×10^{-6} cm
spacing, t	1 cm
2. Objective lens	48" (achromat)
diameter	6"
3. Aperture	
diameter	11/64"
finesse	19.6
4. Instrument field of view	0.2°
5. Interference filter	
diameter	2"
half-width	4.2 Å
peak transmission	45%
peak wavelength	6302 Å
6. Photomultiplier (ITT-FW-130)	
quantum efficiency at 6300 Å	5%
photocathode surface	S-20
effective aperture	1/10"
dark count (cooled to -15°C)	1 count/sec.
(uncooled)	80-90 counts/sec.
7. Resolving power	350,000
8. Operating order	31,700
9. Free spectral range	.198 Å (0.5 cm ⁻¹)
10. Scanning gas	(Dry Nitrogen)
11. Pressure change for 1 order	1.72 psi
12. Overall instrument finesse	11

LIST OF FIGURES

- Figure 1. Michigan Airglow Observatory Schematic
- Figure 2. Fabry-Perot Interferometer Schematic
- Figure 3. Fabry-Perot Interferometer Scanning Mode Schematic
- Figure 4. Neutral Wind Vector Diagram - January 22, 1972
- Figure 5. Neutral Wind Vector Diagram - January 23, 1972
- Figure 6. Neutral Wind Vector Diagram - January 25, 1972
- Figure 7. Neutral Wind Vector Diagram - February 17, 1972
- Figure 8. Neutral Wind Vector Diagram - February 18, 1972
- Figure 9. Neutral Wind Vector Diagram - February 19, 1972
- Figure 10. Neutral Wind Vector Diagram - February 25, 1972
- Figure 11. Neutral Wind Vector Diagram - February 28, 1972
- Figure 12. Neutral Wind Vector Diagram - March 2, 1972
- Figure 13. Neutral Wind Vector Diagram - March 3, 1972
- Figure 14. Neutral Wind Vector Diagram - March 9, 1972
- Figure 15. Interferometric Measurements of Doppler Shifts ($\lambda 6300$)
- Figure 16. Neutral Wind Components - March 2, 1972
- Figure 17. Doppler Profile of $\lambda 7319 \text{ O}^+$
- Figure 18. Arc Scan Temperature - February 17, 1972

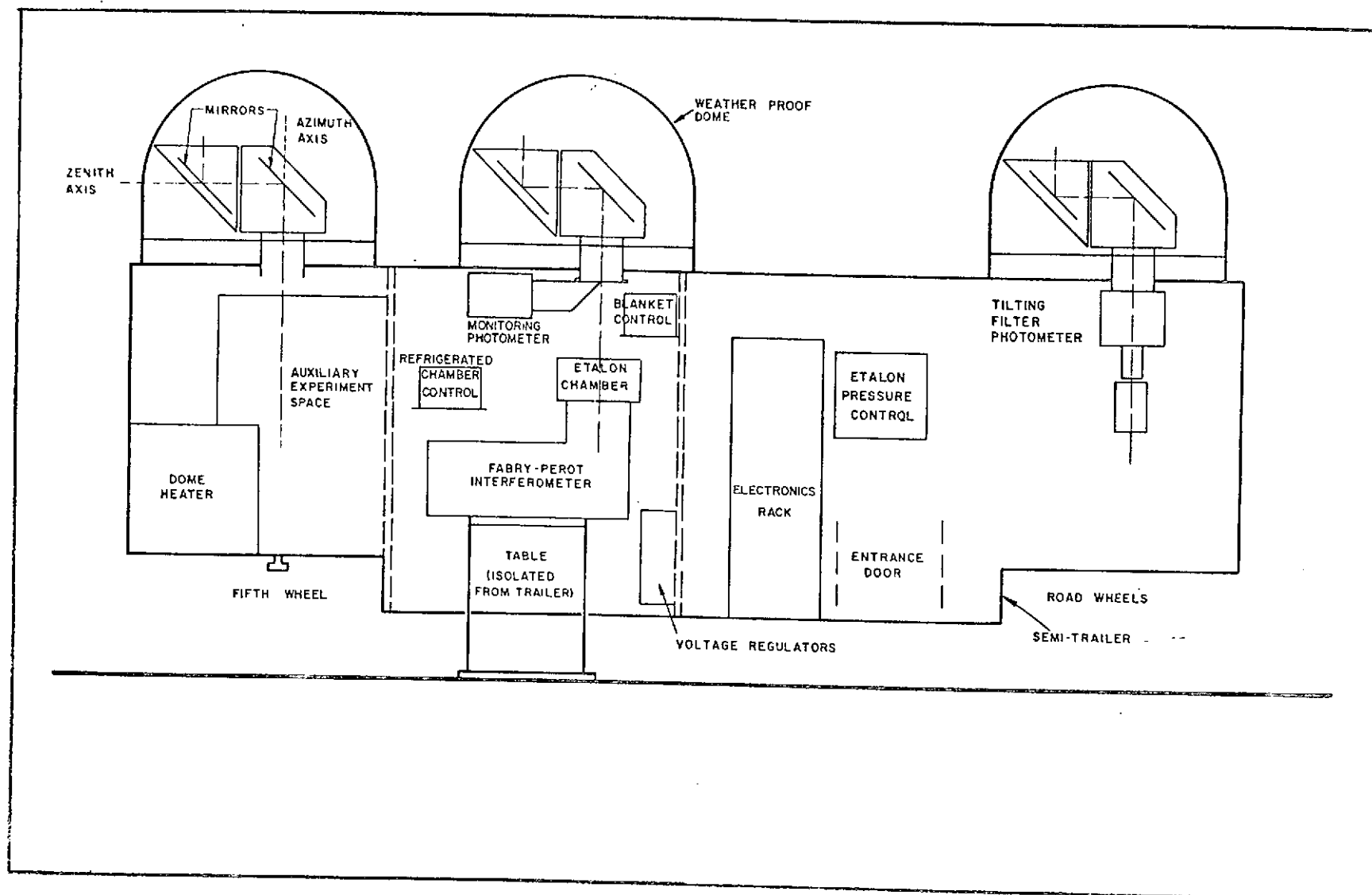


FIGURE 1.
Michigan Airglow Observatory Schematic

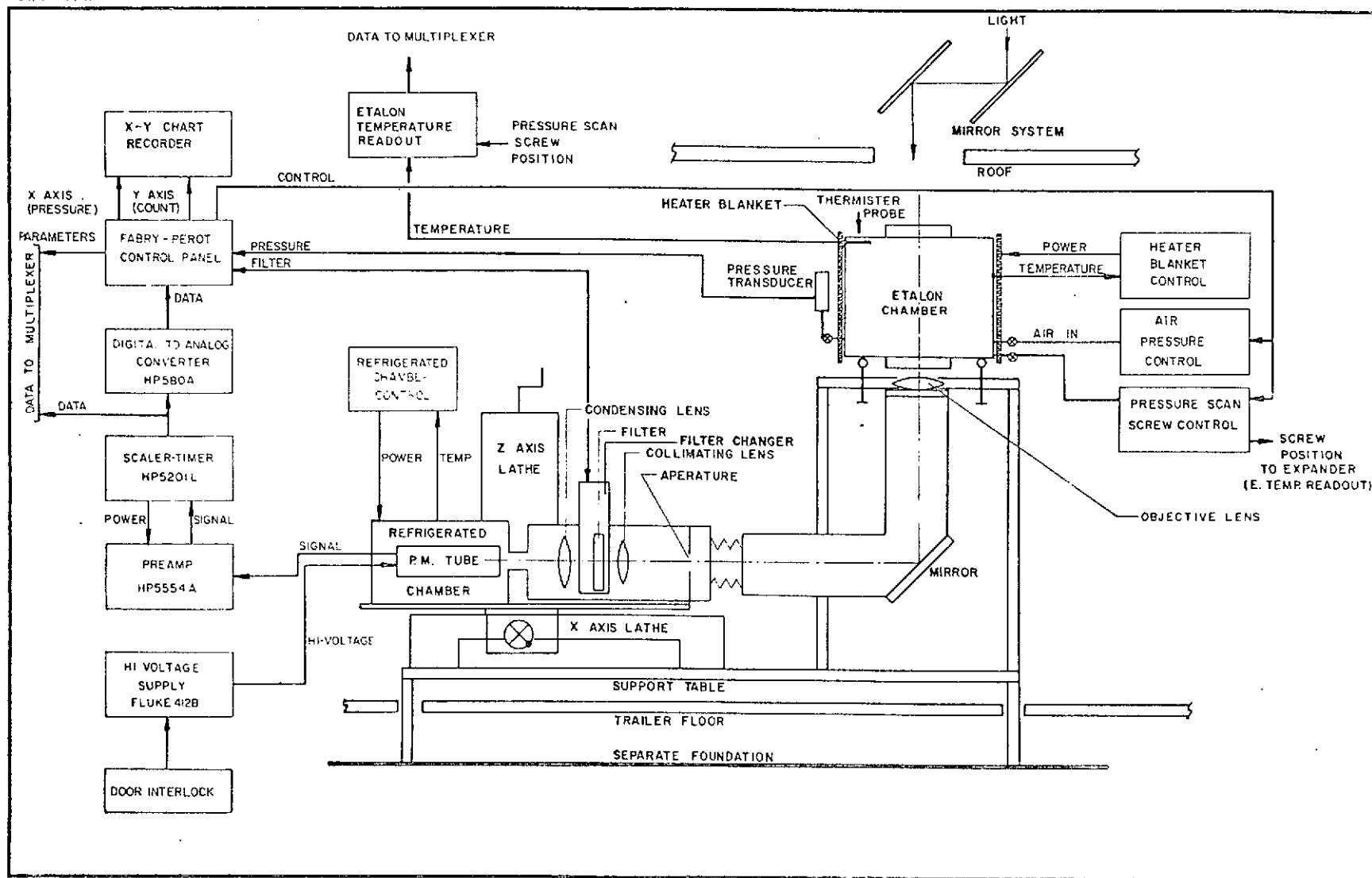


FIGURE 2.
Fabry-Perot Interferometer Schematic

FIGURE 3.
Fabry-Perot Interferometer Scanning Mode Schematic

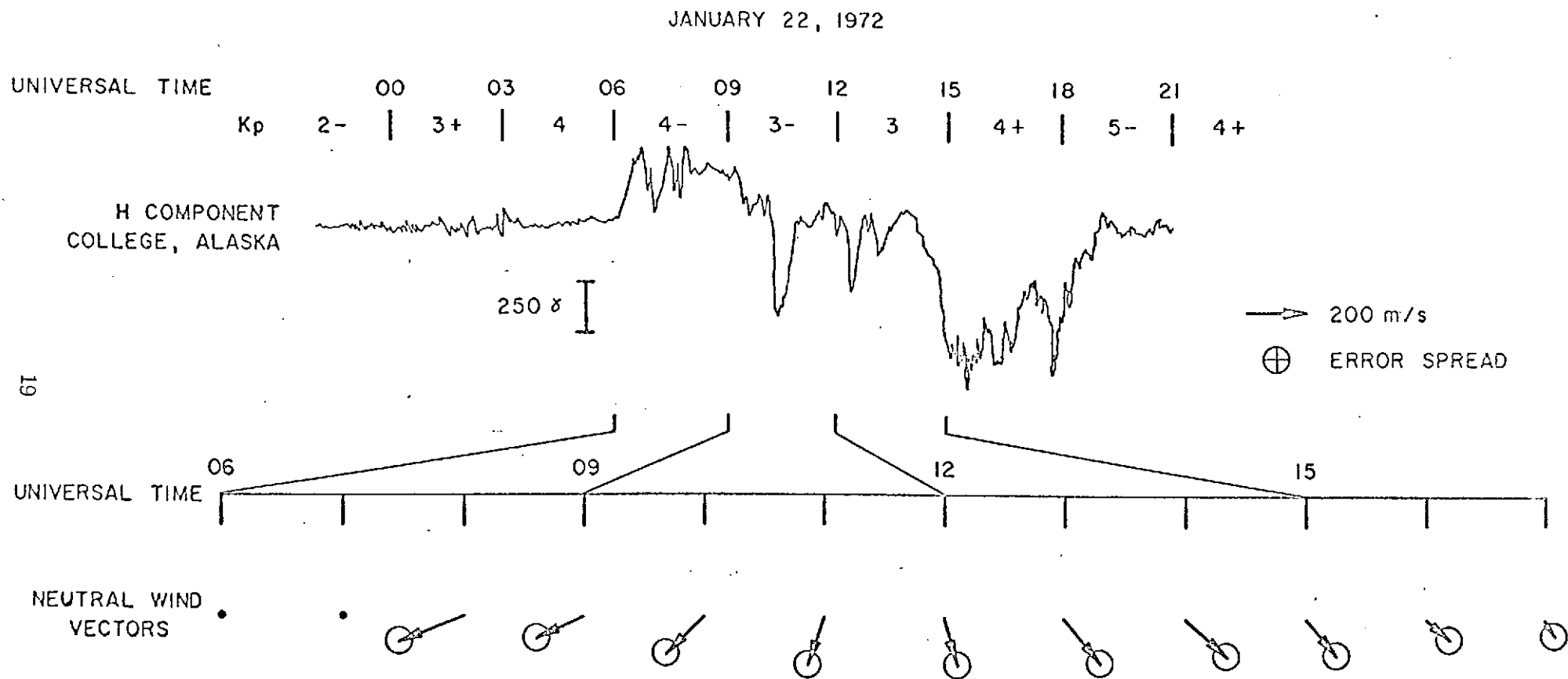


FIGURE 4.
Neutral Wind Vector Diagram

JANUARY 23, 1972

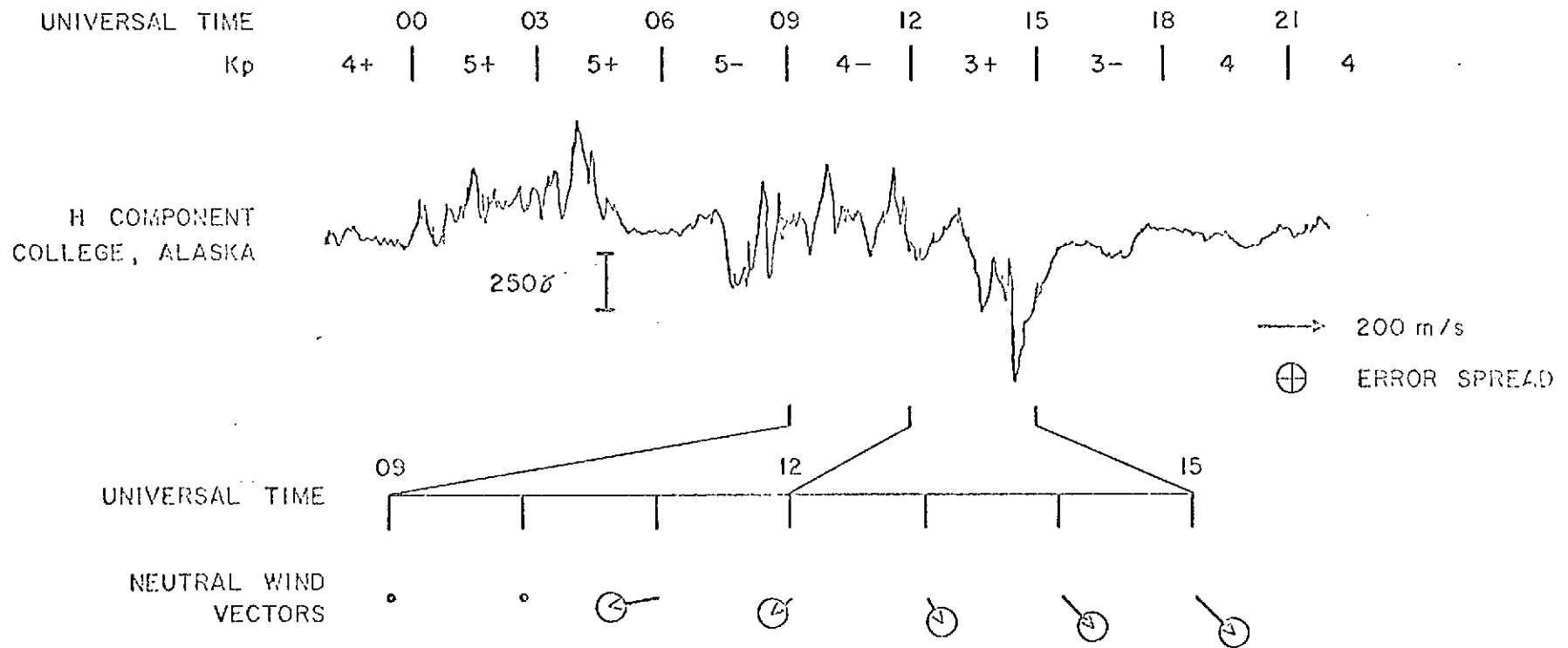


FIGURE 5.
Neutral Wind Vector Diagram

JANUARY 25, 1972

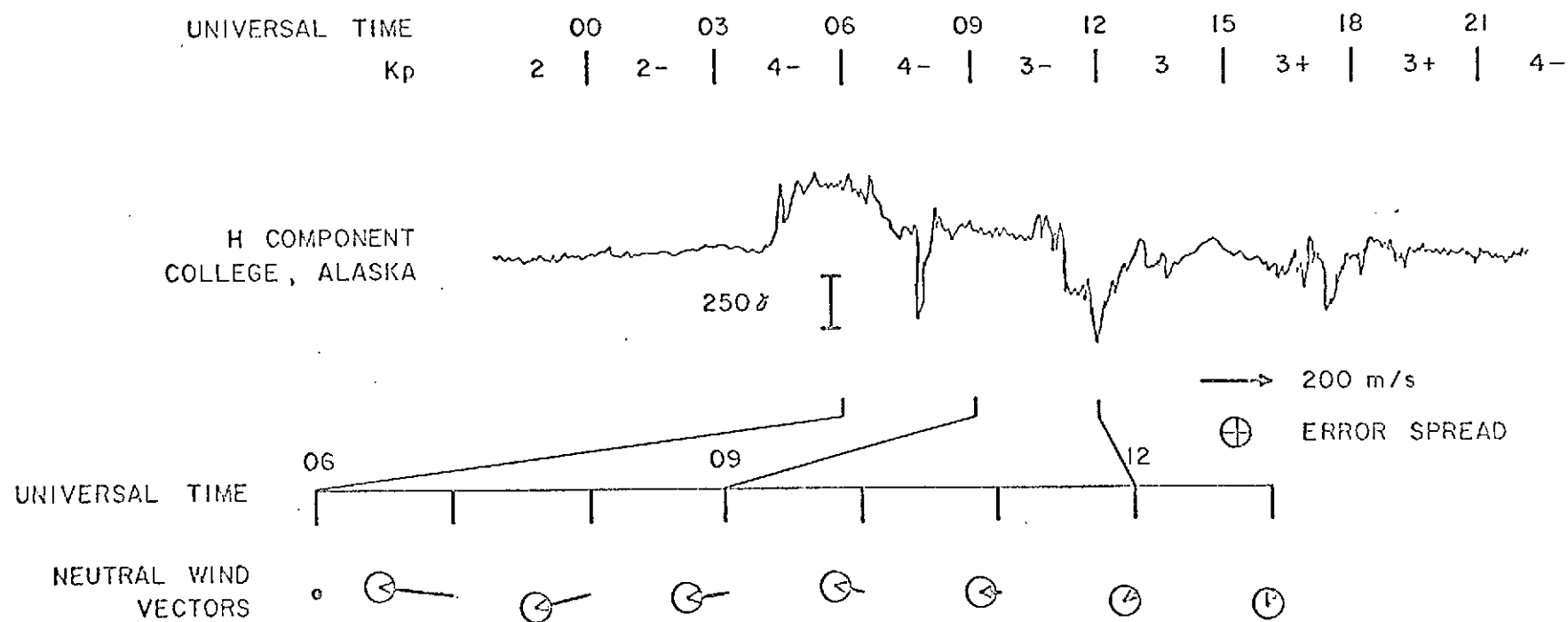


FIGURE 6.
Neutral Wind Vector Diagram.

22

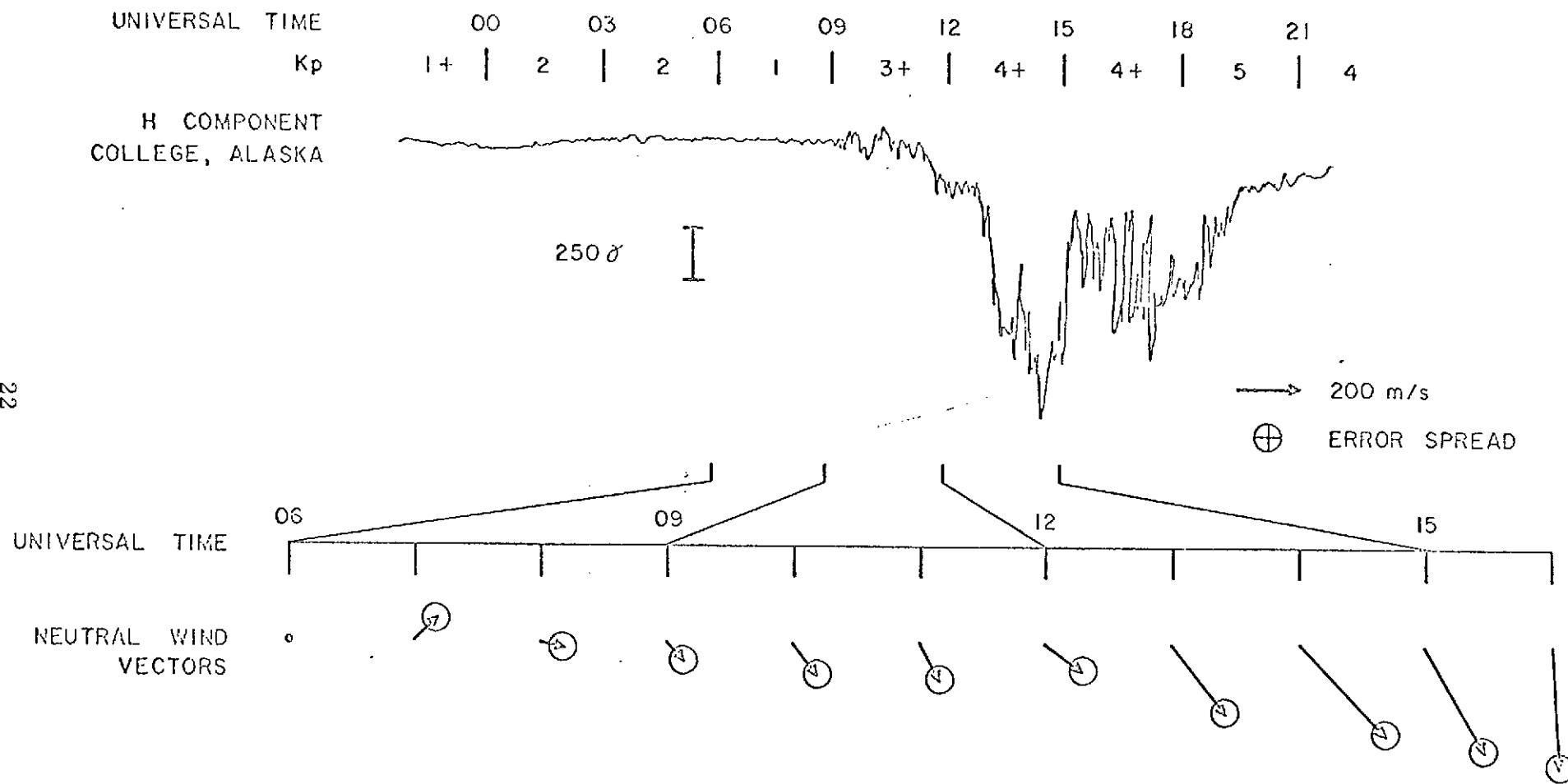


FIGURE 7.
Neutral Wind Vector Diagram.

FEBRUARY 18, 1972

UNIVERSAL TIME 00 03 06 09 12 15 18 21
Kp 4 3- 3 3 1- 0 0+ 1 5-

H COMPONENT
COLLEGE, ALASKA

250 γ

→ 200 m/s

⊕ ERROR SPREAD

UNIVERSAL TIME



NEUTRAL WIND
VECTORS

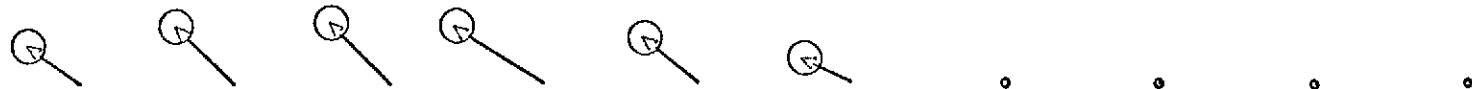


FIGURE 8.

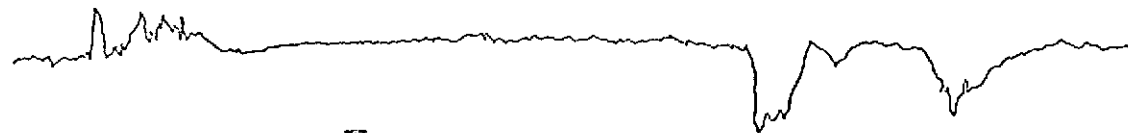
Neutral Wind Vector Diagram.

FEBRUARY 19, 1972

UNIVERSAL TIME
Kp

00 03 06 09 12 15 18 21
5- | 5+ | 2+ | 1 | 0+ | 3- | 3 | 3- | 2-

H COMPONENT
COLLEGE, ALASKA



250γ

→ 200 m/s
⊕ ERROR SPREAD

24

UNIVERSAL TIME

06 09 12 15

NEUTRAL WIND
VECTORS

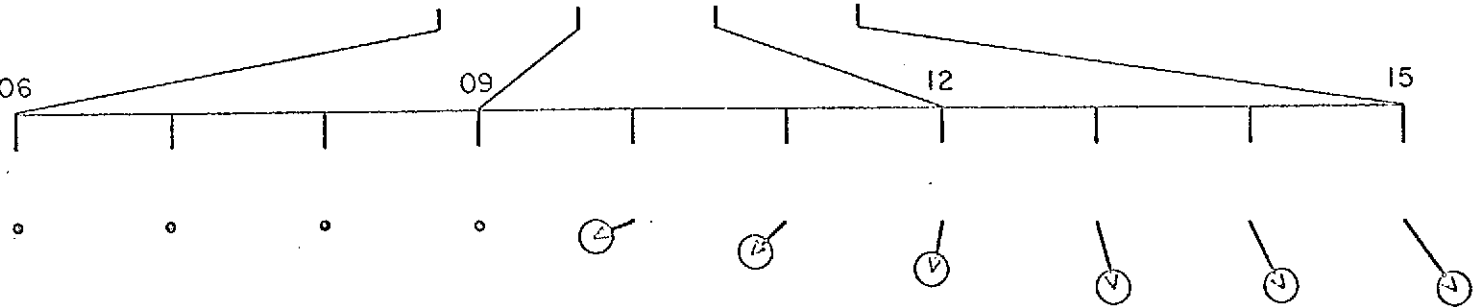


FIGURE 9.
Neutral Wind Vector Diagram.

FEBRUARY 25, 1972

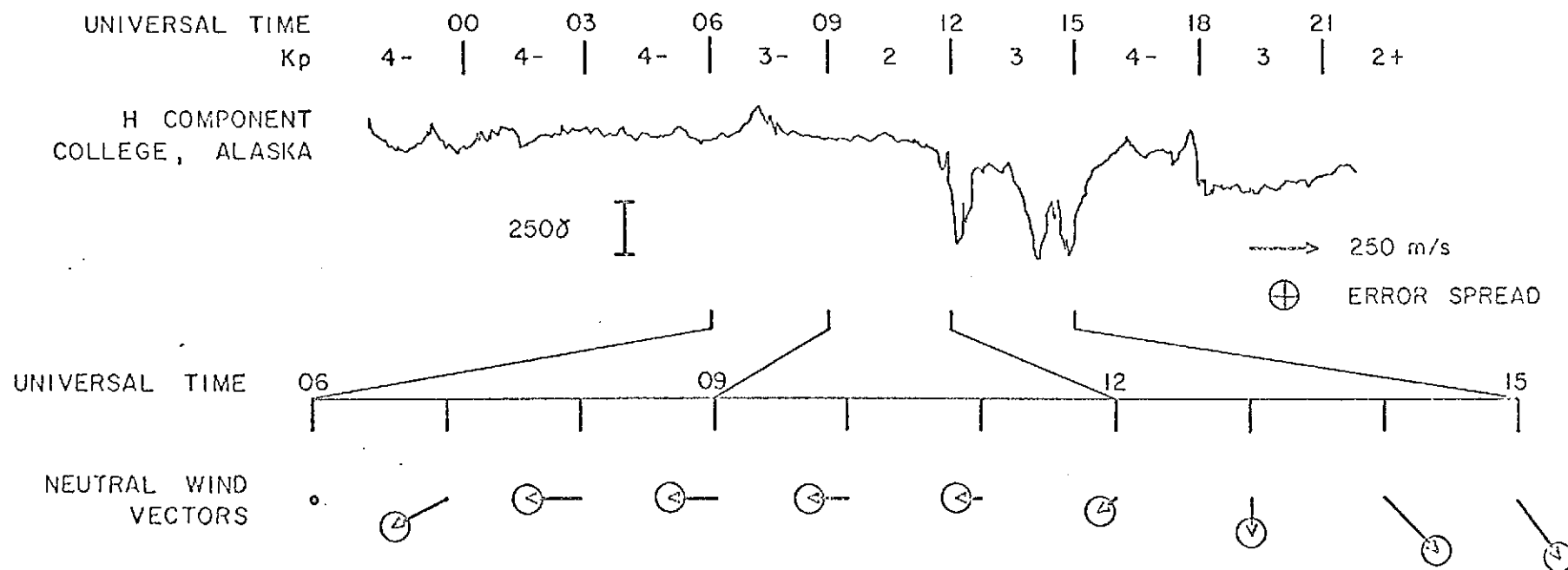


FIGURE 10.
Neutral Wind Vector Diagram.

FEBRUARY 28, 1972

UNIVERSAL TIME

00	03	06	09	12	15	18	21	
Kp 3-	2-	3-	2	1	1-	0+	2-	1+

H COMPONENT
COLLEGE, ALASKA



250γ I

→ 250 m/s

⊕ ERROR SPREAD

UNIVERSAL TIME

06 09 12 15

NEUTRAL WIND
VECTORS

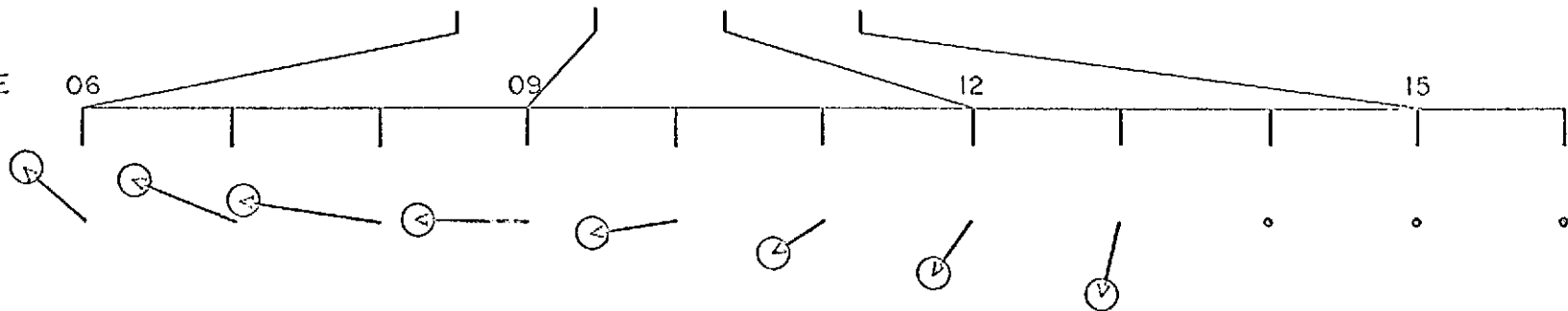


FIGURE 11.
Neutral Wind Vector Diagram.

COMPARISON OF NEUTRAL WIND VECTORS WITH THE COLLEGE MAGNETOGRAM

MARCH 2, 1972

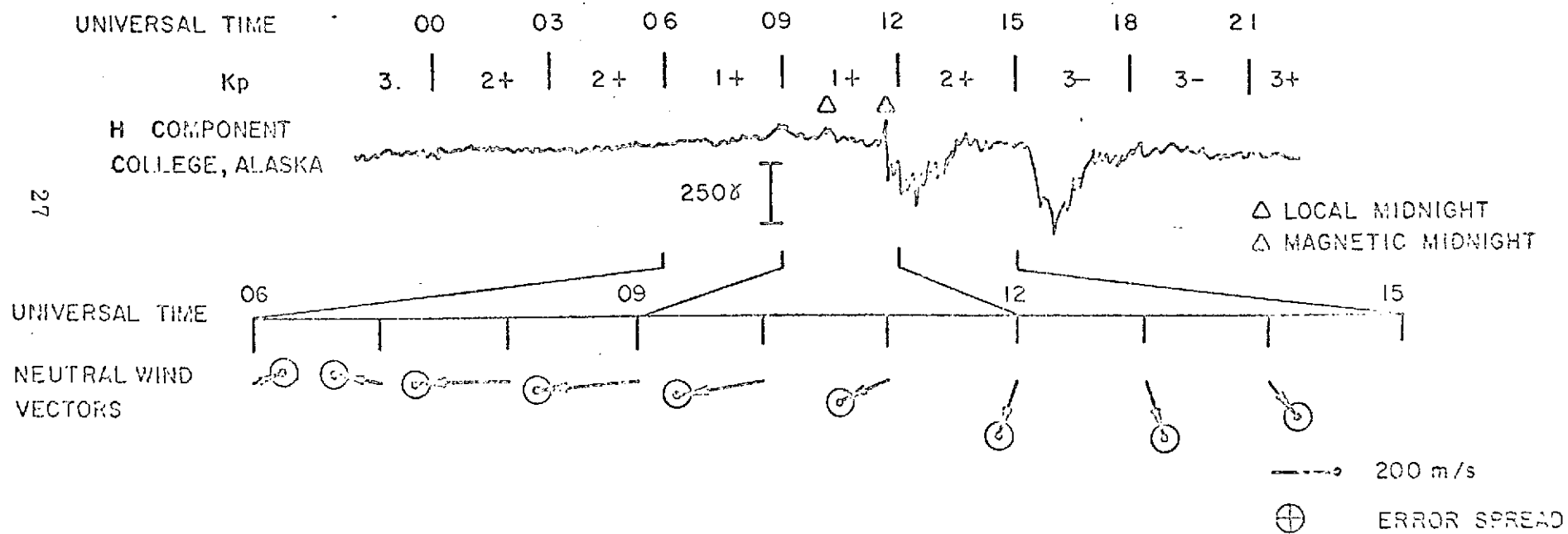


FIGURE 12.
Neutral Wind Vector Diagram.

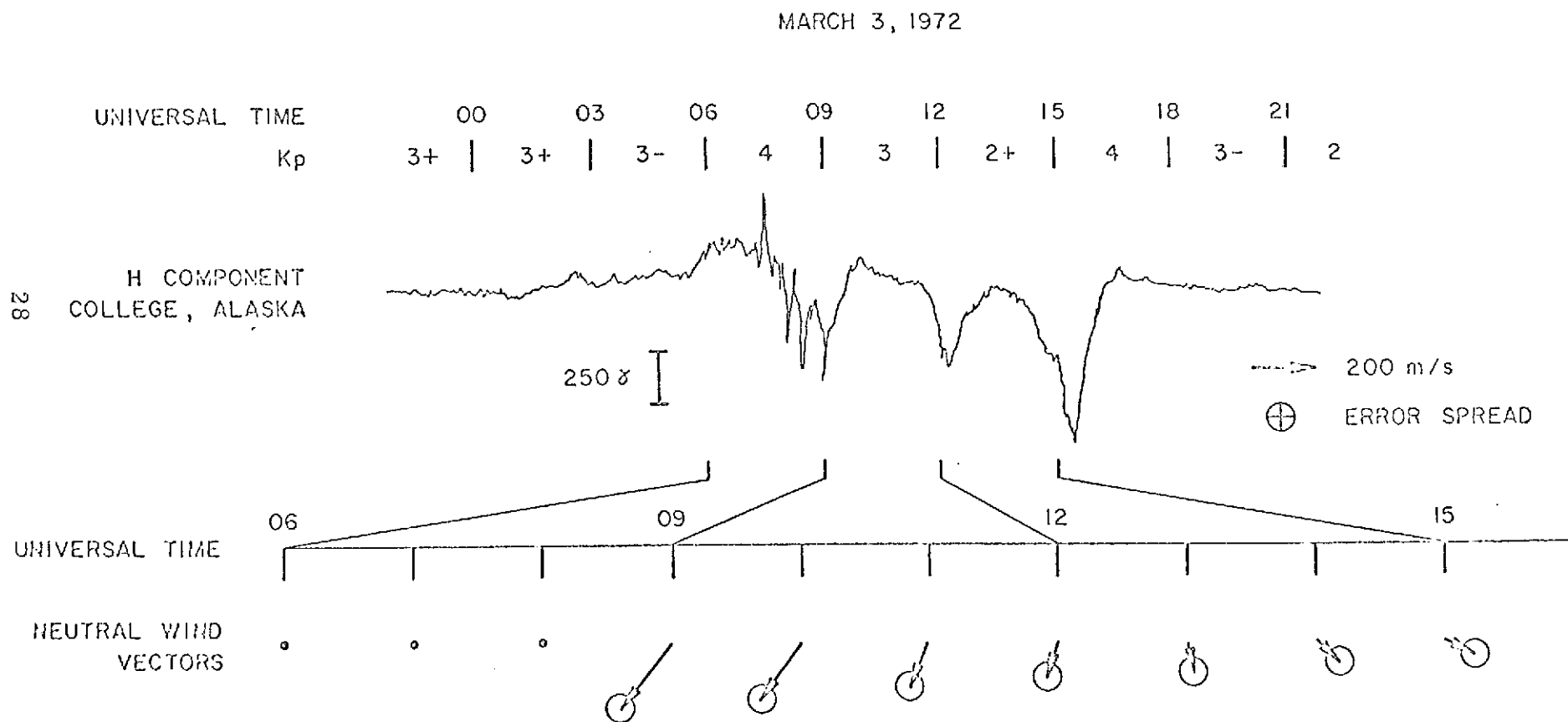


FIGURE 13.
Neutral Wind Vector Diagram.

COMPARISON OF NEUTRAL WIND VECTORS WITH THE COLLEGE MAGNETOGRAM MARCH 9, 1972

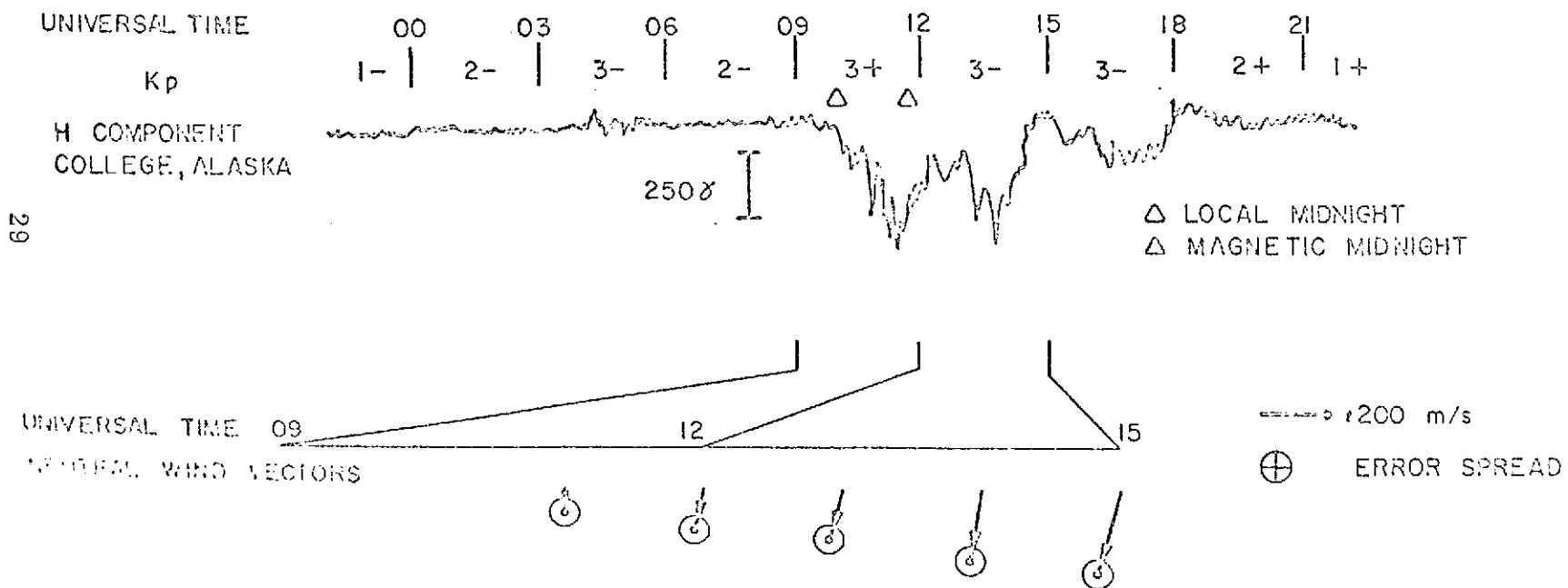
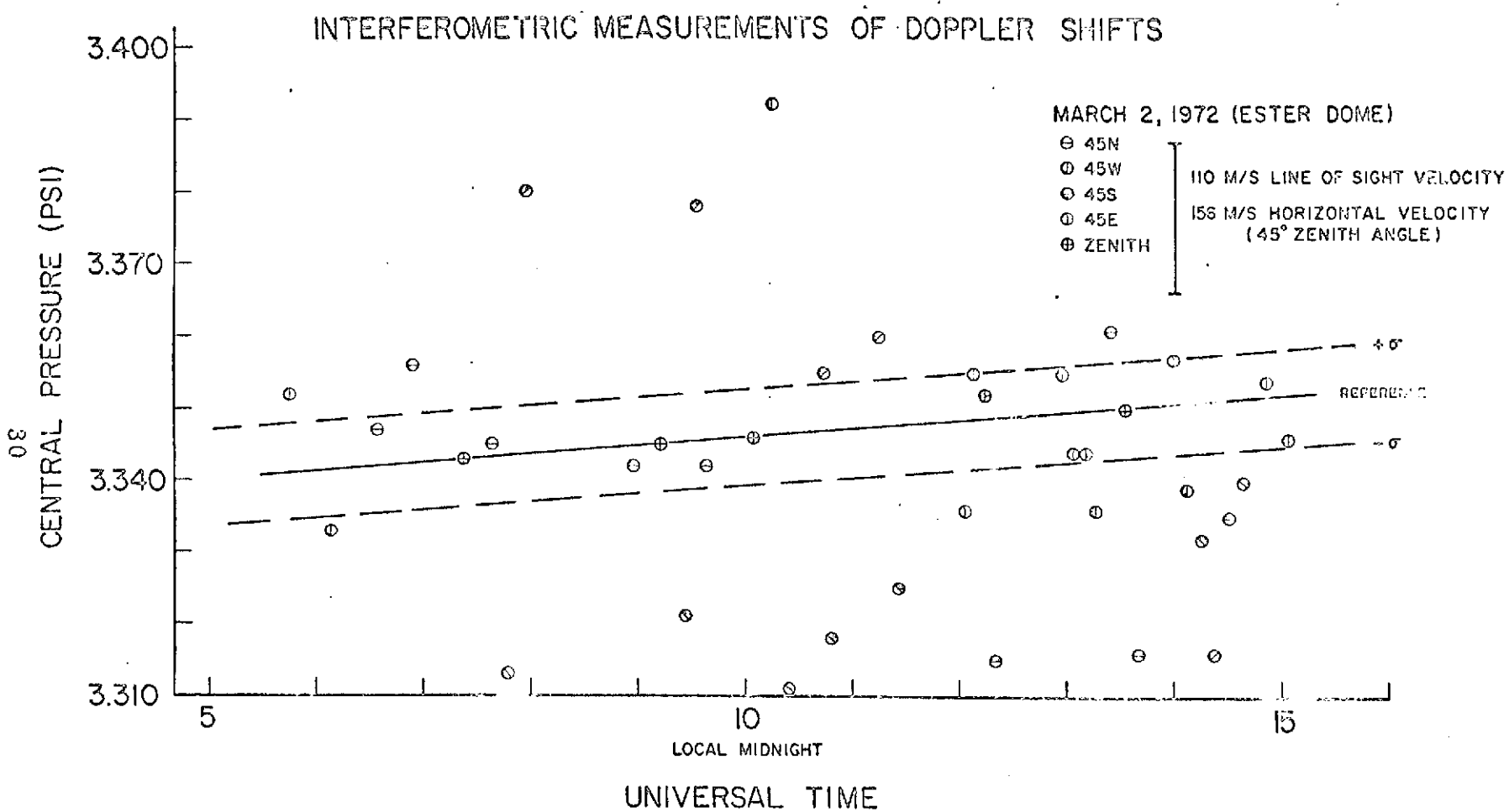


FIGURE 14.
Neutral Wind Vector Diagram.



NEUTRAL WIND COMPONENTS
MARCH 2, 1972
ESTER DOME COLLEGE, ALASKA

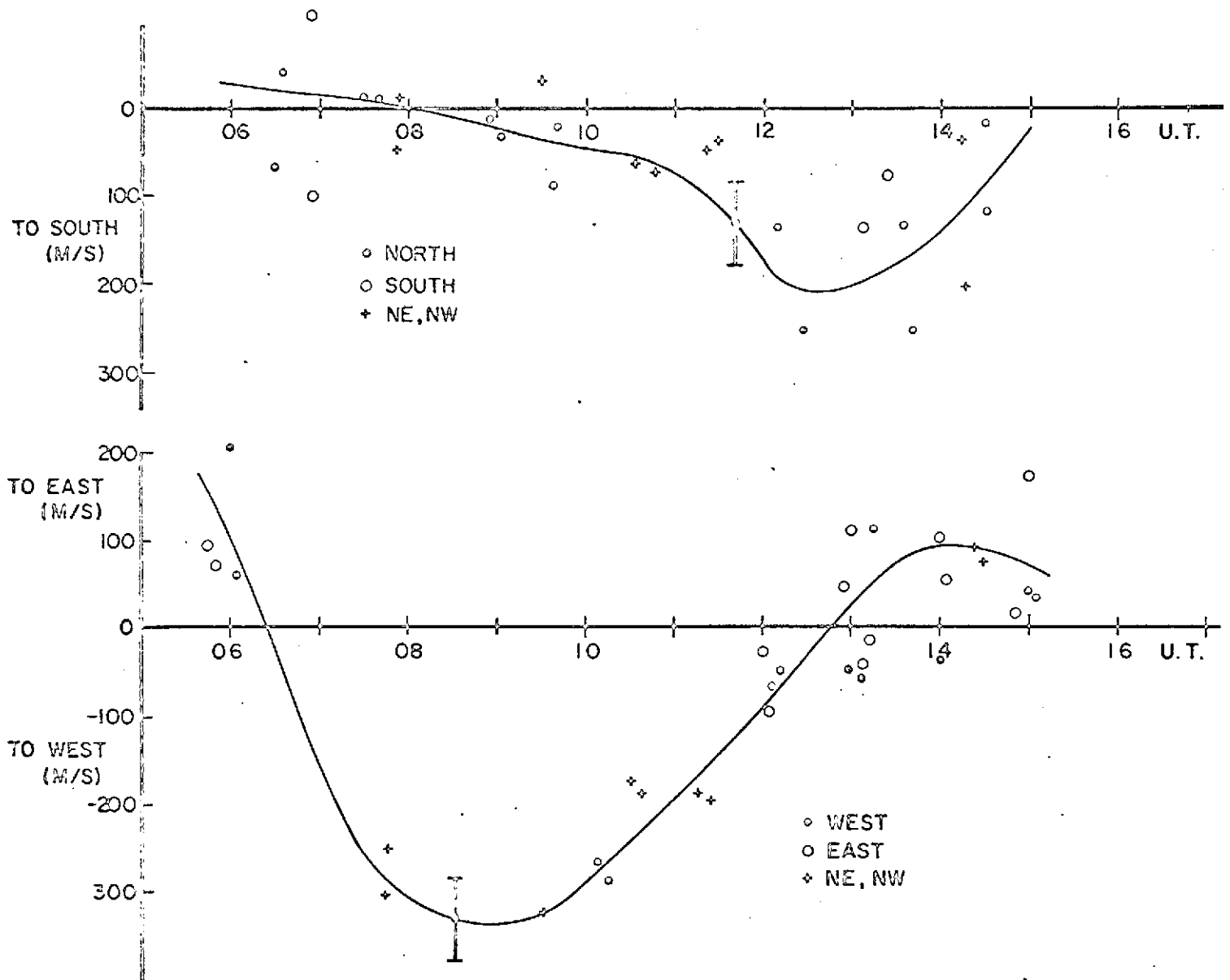


FIGURE 16.

FEBRUARY 12, 1972 (AST) DOPPLER PROFILE OF $\lambda 7319$ 0°

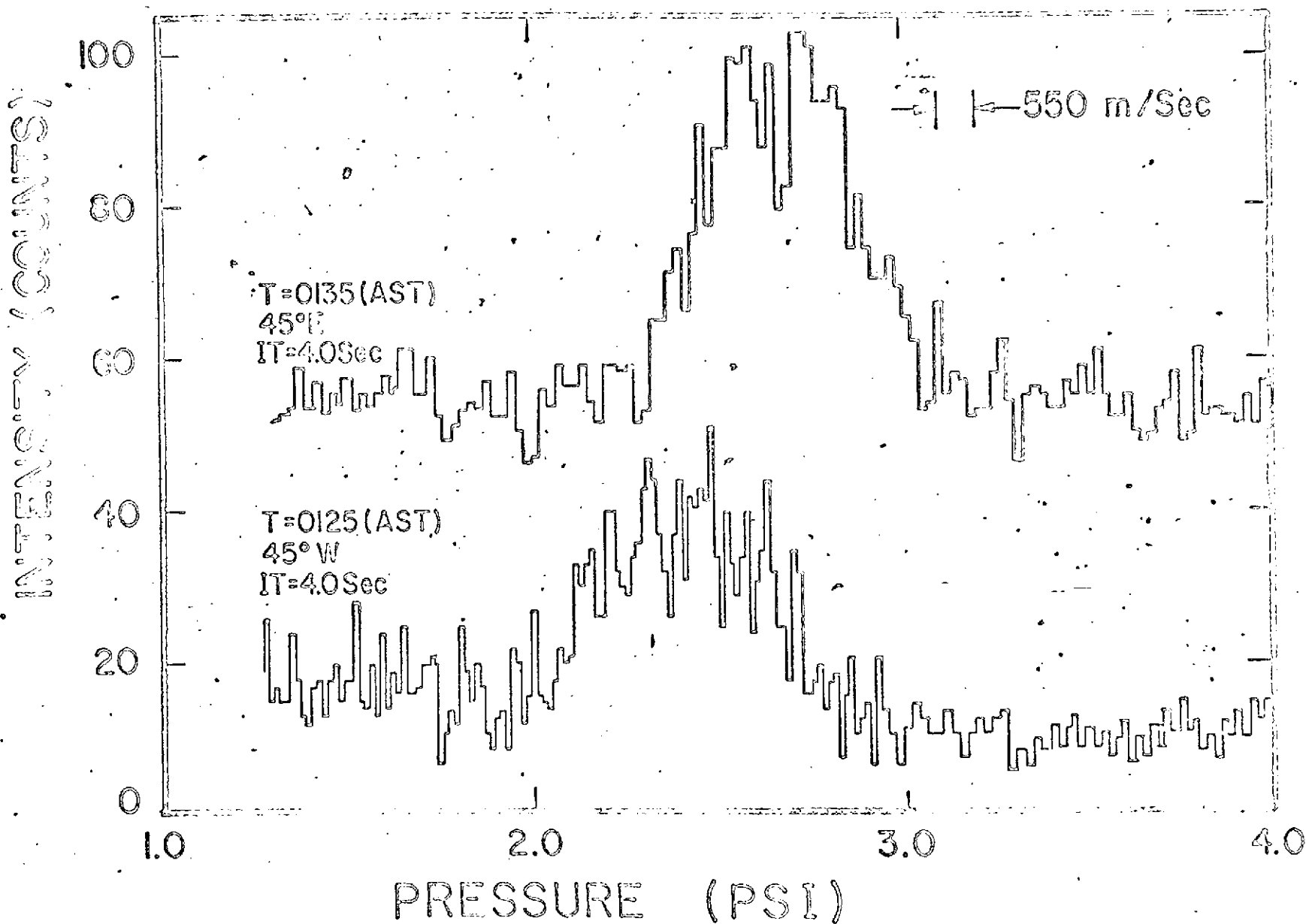


FIGURE 17.

ARC SCAN TEMPERATURE (FEBRUARY 17, 1972)

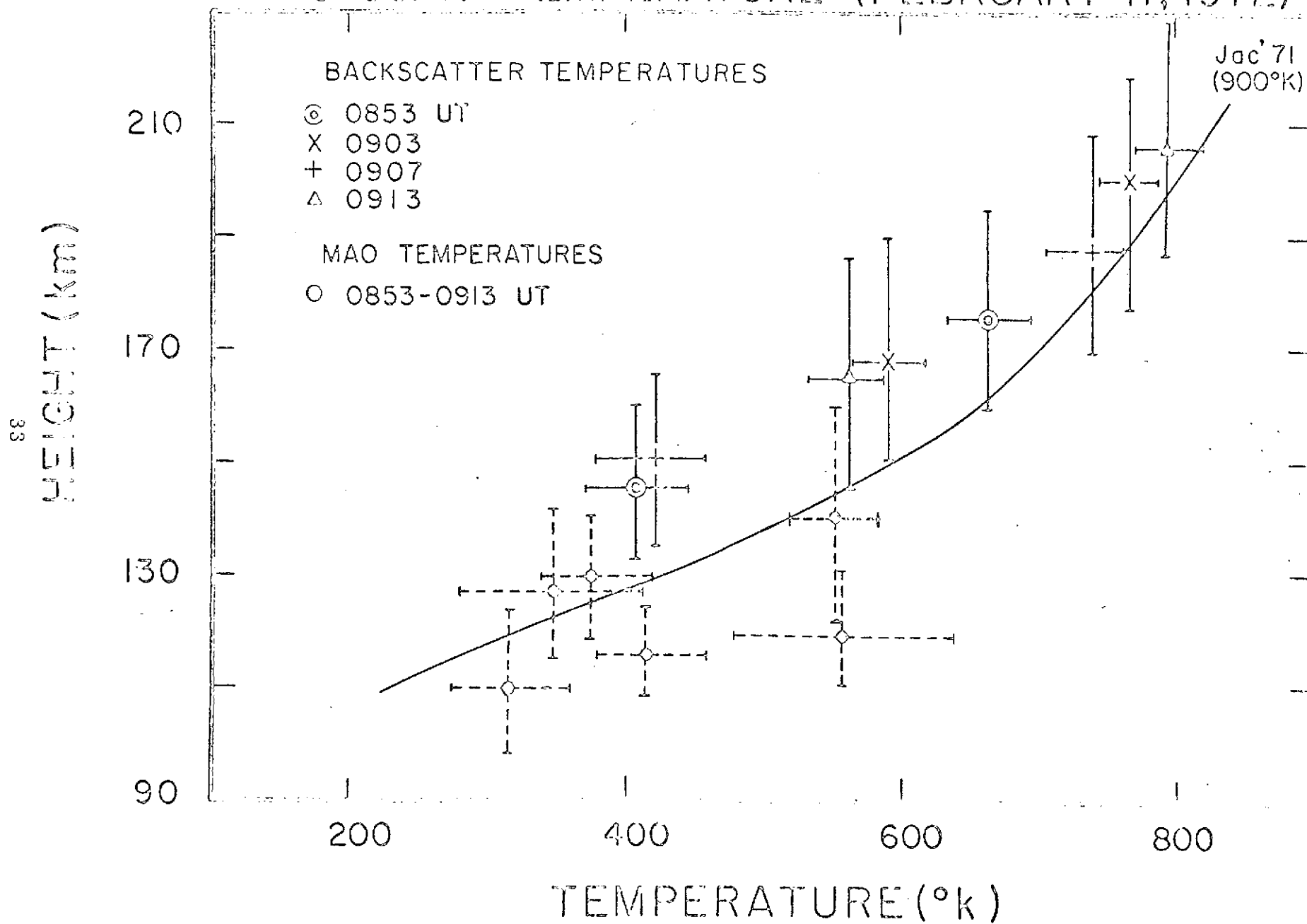


Figure 18.

APPENDIX A

SUMMARY 1971 - 1972 OBSERVATIONS

MAO was operational in the first week of December, 1971.

Work below describes the observational work that began in January 1972.

The array of instrumentation was the following:

MAO

6 inch Fabry-Perot interferometer

4 channel tilting filter photometer

3 axis fluxgate magnetometer

TV monitor of red channel of color TV system manned by
Geophysical Institute personnel.

University of Colorado

1/2 m Ebert-Fastie spectrometer (operated by Fred Rees)

University of Alaska (Geophysical Institute)

1 35mm ASC (operated upon demand)

1 16mm ASC (operated continuously)

Meridian scanning photometer (Gerald Romick)

3/4 m Fastie-Ebert spectrometer (V. Degan)

TV color system (Neil Davis)

Measurements of λ 7319 were obtained upon a number of occasions, but most notably upon February 12 and February 19, 1972.

Dates upon which neutral wind measurements on red and green O lines were made are the following: (Universal dates). Asterisk denotes good coverage.

January 14, 15, 21*, 22*, 23, 24*.

February 3, 13, 14, 15, 17*, 18*, 19*, 21, 25*, 28*.

March 1, 2*, 3, 4, 5, 6, 7*, 8, 9*, 15, 31*.

April 1*, 2*, 3, 6.

Fabry-Perot sodium measurements were made on March 11, 12, 13, 14, 17, with both 1 cm and 1.5 cm spacers. Data not yet reduced.

Scanning gas was changed to SF6 on March 23(UT) and 1/4 cm spacer inserted. H_{α} and λ 7319 measurements were made on March 23. The neutral wind measurements on March 24, 25, 26, 27, were made to test a technique where the FP was positioned at the fringe half height and a very slow almucantar scan was initiated. The problem with this technique is that background shifts due to aurora or moonlight present a severe analysis problem.

LOCAL DATES	MAO ACTIVITY FOR WINTER 1973
Feb 2/3, 1973	Setup of FP; checkout of both photometers coordinate work of t.f. photometer with Gary Swenson
Feb 3/4	Further checkout of FP. No data.
Feb 4/5	Sensitivity work on 5577; sky work, 70°N. Very little wind found.
Feb 5/6	Red line sensitivity work; cycling around, found indications of meridional gradients.
Feb 6/7	Hg calibration
Feb 7/8	Zenith run in $\lambda 6300$. First indication of vertical fluctuations. Variable integration times ($C_p=10,000$)
Feb 8/9	Zenith run in $\lambda 6300$ with frequent checks against Ar lamp. More vertical fluctuations noted. ($C_p=4000$)
Feb 9/10	N,S measurements in $\lambda 6300$. $C_p=4000$ Wind sensitivity study in $\lambda 6300$
Feb 10/11	Ar, Hg calibration study
Feb 12/13	N,S measurements upon a quiet night in $\lambda 6300$
Feb 13/14	N,S measurements in $\lambda 6300$ ($C_p \approx 4000$)
Feb 14/15	Ar-Hg calibration study - hysteresis study by rapid counting
Feb 15/16	Zenith, north fringes, $\lambda 6300$
Feb 19/20	Ar/Hg study (8 hours run)
Feb 21/22	Zenith, W and N fringes in $\lambda 6300$. First day of active aurora sequence. Haze and clouds forced early termination of work.
Feb 22/23	Cycling around with good statistics, red line. Active aurora. Found increase of $\lambda 5577$ in photometer factor of 3 as a result of optimization. Point of this night's work in red line was to look for gradient effects from pairs of N-S and E-W measurements, concentrating upon good statistics.

Feb 23/24	Zenith study of red line during active auroras. Work terminated with E,W,N,S measurements to look for a zero.
Feb 24/25	Cycling around in $\lambda 6300$. Active auroras all night.
Feb 25/26	Coordinated zenith run with radar. Zero sought by E,W,N,S runs. Hg calibration.
Feb 26/27	Coordinated cycling around with the radar.
Feb 27/28	Cycling around
Feb 28/Mar 1	North and zenith scans in conjunction with the radar run in magnetic zenith
Mar 1/2	No data-Ar calibration study
Mar 2/3	Cycling around
Mar 3/4	West sequence; skies a bit hazy. Quiet night
Mar 6/7	Cycling around; hazy skies at end
Mar 7/8	Calibration work. Cloudy
Mar 9/10	More calibration work. Cloudy
Mar 10/11	A little zenith work
Mar 11/12	Cycling around until 0030. Zenith work to look for fluctuations. Hazy skies. Lifted mirror at 0300 to see if scattering is a problem
Mar 14/15	Ar run, 7 hours
Mar 15/16 No radar data	Mostly 50° North run. Night may be useful for meridian arc scans in $\lambda 6300$ when the aurora moved through the field of view. Active auroras, breakup around 0030 AST. Wind to the south after breakup
Mar 16/17	Hg calibration
Mar 17/18	50° W for entire night. Meridian scans with photometer during ISIS II satellite pass at 0028 AST. Definite wind to west with a shift to east after breakup around 0200 AST. Full moon. 1000 γ negative bay at 0200 AST. Pulsating aurora.

Mar 18/19 Zenith study in $\lambda 6300$. Tilting filter photometer backing up FP to see if background of $\lambda 6300$ can be related to fluctuations (i.e., strong auroras create background shift that affects relative sensitivities of FP and tracking photometer. Lots of aurora, 1500 γ negative bay. Made occasional looks to west and north to determine nature of wind pattern while doing zenith study. No radar data.

Mar 19/20 Cycling around. Very active evening. No radar data.

Mar 20/21 Heppner first flight at 0600 UT. 200 γ positive bay. Cycling around in support to measure neutral wind. Zenith study alternating between $\lambda 5577$ and $\lambda 6300$ to look for fluctuations. Radar cycling until 1520 UT. 3PV. 10 min IP. FLP included.

Mar 21/22 Heppner second flight. Cycled around in support. Radar doing 3PV until 0710 UT. Then 3PV(SRI) until 1343 UT. Then up the field line from 1344 to 1432 UT. Continued cycling until 0150 AST. Clouds and haze until 0300 AST. Did N-S, Z=0 in conjunction with radar; found wind to the south at 0300 AST so radar went to magnetic zenith while FP did N, Z=0 scans. Radar saw indications of vertical ion drifts (at 210 km) in conjunction with 300 m/s (guess) wind to the south.

Mar 22/23 Cycles around until 0130 AST. Then coordinated measurements with radar in N-S, Z=0 direction to look for gradient effects. Radar and MAO found motion to south. Radar doing 3PV between 0645-0910 UT. North until 1200 UT. N,S scans between 1200 UT-1415 UT.

Mar 23/24 Cloudy. Some tilting filter photometer data from zenith in early evening. Radar doing 3PV (MZ included). 0700-1139 UT. 1242-1600 UT, 3PV.

Mar 24/25 Coordinated measurement with radar. Found N-S fluctuations of drift in coordination with radar (ion wind to the north followed with neutral wind to north; ion wind to south followed with neutral wind to south). Cycling around during breakup until 0340 AST. Radar looked north until 0040. Then did east and north measurements until 0255 AST.

Mar 25/26 Cloudy. Primarily Ar/Hg calibration work. Radar did 3PV, 0709 to 1253 UT.

Mar 26/27 Very quiet initially, tilting filter photometer meridian scans for Vince. Calibration with Kofsky's source. N, Z=0 work with radar on magnetic zenith. Heppner's third flight. Cycling around in support; peculiar E-W behavior, but very low speeds. Radar began N, MZ meridian scans for conjugate photoelectron flux from 0728 to 0928 UT. 3PV until 1115 UT. 1118-1200 UT, MZ. Mostly E thereafter.

Mar 27/28 Radar looked north from 0725-0734, looked south from 0734 to 0744. Then MZ until 1141. North and zenith measurements with occasional looks E and W.

Mar 28/29 Hg/Ar study; λ 6300 geog. zenith measurements at end.

Mar 29/30 Geog. zenith study in red line. Dome removed and mirror swung back. Sensitivity study, red line. Radar looking west from 0749 UT to 1220 UT. Cycling around until 1359 UT.

Mar 30/31 Geog. zenith study in green line. Very low activity produced considerable scatter so results inconclusive. Should be useful night for E-region temperatures in quiet conditions. Radar did 3PV from 0218 UT to 0908 UT. N, S(45°Z) from 0709 to 1153 UT. 1205-1420 UT radar looked west with a couple of checks in the north.

Mar 31/Apr 1 λ 5577 geog. zenith study with good statistics until arc passage in zenith. Until 0030 AST broke off for tracking photometer--FP X-Y arc scans until 0130. Found hysteresis loops indicating temperature effects. Determined that method of data reduction slightly sensitive to temperature. Radar did 3PV cycle between 0729 to 0859 UT. Then magnetic zenith until 1641 UT.

Apr 1/2 Hg calibration, cloudy initially.

Apr 2/3 λ 5577, λ 6300 wind sensitivity studies. Clouds and haze present.

Apr 3/4 Magnetic zenith study in λ 5577. Arc scan at 2300 in coordination with Romick. Some vertical fluctuations found in λ 5577. Sensitivity study in 5577. T.F. photometer in rocket position all night. Radar in mag. Z 0753 to 0810 UT. 3PV from 0823 to 1040 UT. Off afterwards.

Apr 4/5 Coordinated measurements with the radar; both systems looking west 45°. Found ion and neutral drifts to the west that died away together. Radar from 0632 to 0730, 236 Rg 70° elev; 0705 - 1102, 45° N (mag). 3PV from 1105 to 1247 US. Then 13 min more of mag. west.

Apr 5/6 Hg/Ar study with statistics that equivalent to the sky. No fluctuations observed.